POLITYKA ENERGETYCZNA – ENERGY POLICY JOURNAL

2026 ✦ Volume 29 ✦ Issue 1 ✦ 171–204

DOI: 10.33223/epj/211850

Renganathan Rani Hemamalini[1]

Enhancing power matching and extraction in hybrid renewable energy systems through HawkDeep Gradient Fuzzy Recurrent Control

Abstract: Hybrid renewable energy systems are one of the highly suitable solutions for the growing energy demand. However, the performance of this system is significantly affected by the power imbalance, unstable DC-bus voltage, and reduced system efficiency. To overcome these issues, a novel HawkDeep Gradient Fuzzy Recurrent Control framework is proposed. This method is used to optimize the management of power characteristics and stabilize the system performance in High Renewable Energy Systems. Moroever the current control algorithms frequently rely on predefined rules, which are not flexible enough to deal with sudden and erratic variations in load demands and power generation. To resolve this, an Intelligent Hawk Fuzzy Control Algorithm is proposed, which integrates fuzzy logic with Reflective Quasi-Hawk Optimization to rapidly get the best answers, thereby guaranteeing the balanced power supply and demand even in the event of sudden inrush currents. Furthermore, the mismatch in ramp rates causes temporary power imbalances and instability in the direct current bus voltage, stressing the system and reducing efficiency. Therefore, a Deep Recurrent Policy Gradient technique is introduced, which integrates Gated Recurrent Units with Deep Deterministic Policy Gradient. The method optimizes control actions for stable power regulation in which the Gated Recurrent Units deal with temporal dynamics to rectify ramp rate

✉ Corresponding Author: Renganathan Rani Hemamalini; e-mail: ranihemamalini.eee@spiher.ac.in

[1] St. Peter Institute of Higher Education and Research, Avadi. Chennai 600077, India; ORCID iD: 0000-0001-8510-034X; e-mail: ranihemamalini.eee@spiher.ac.in

discrepancies and power imbalances in multiport direct current converters. Experimental results demonstrate that the proposed model achieves an accuracy of 0.98 and a net output power of 72.1kW under variable conditions, ensuring efficient and stable operation at medium-scale power levels.

Keywords: microgrid stability, converters, photovoltaic panels, alternative energy, decentralized energy generation

Terminology

$Crisp_{(t)}$	–	crisp control action at time (t)
$Member_{Degree_i}$	–	membership degree of the i-th fuzzy rule
Out_i	–	output value corresponding to i-th fuzzy rule
$Pos_{(t)}$	–	position vector of a hawk
$Pos_{b(t)}$	–	best hawk's position at time
$Pos_{avgloc(t)}$	–	the average location of every position
$rand_1$, $rand_2$, $rand_3$, $rand_4$, $rand_5$	–	random variables
L_{limit}	–	lower bound of parameter space
U_{limit}	–	upper bound of parameter space
$Energy_{cs}$	–	current escape energy at iteration
$Energy_{initial}$	–	initial escape energy
$t_{current}$	–	current iteration
t_{total}	–	total number of iterations
J_{esc}	–	random escape power
X^{qr}	–	candidate solution generated by quasi-reflection
af_{up}^{t}	–	update gate input for GRU at time (t)
w_{if}	–	input feature weights for GRU gates
G_{up}^{t}	–	update gate output at time (t)
w_{hs}	–	hidden state features
w_{ireset}, w_{hreset}	–	reset gate weights
$w_{i_{h'}}$ h', $w_{h_{h'}}$	–	candidate hidden state weights
$\varnothing$	–	α non-linear activation function
$L(\theta_M)$	–	loss function of value function
a_{rg}^{t}	–	reset gate input at time (t)
$a_{h'}^{\sim t}$	–	candidate hidden state input
G_{h}^{t}	–	candidate hidden state
$G_{h'}^{\sim t}$	–	hidden state
G_{h}^{t-1}	–	previous hidden state
st_j	–	state variable

ac_j – action variable
re_j – reward variable
γ_{dis} – discount factor
$\mu(s_{tt})$ – batch size at each update
HRES – Hybrid Renewable Energy System
PV – Photovolatic
SVMs – Support Vector Machine
NNs – Neural Networks
LSTM – Long Short-Term Memory
RNNs – Recurrent Neural Networks
GRU – Gated Recurrent Units
RQHO – Reflective Quasi-Hawk Optimization
DDPG – Deep Deterministic Policy Gradient
TSR – Tip Speed Ratio
OT – Optimal Torque
MPPT – Maximum Power Point Tracking
P&O – Perturb and Observe
IC – Incremental Conductance
PMSG – Permanent Magnet Synchronous Generator
HRDS – Hybrid Distributed Generation System
PQ – Power Quality
FBS – Fleeting Bird Search
WP – Wind Power
SMC – Sliding Mode Control
APOAM – Adaptive Perturbation and Observation Algorithm Method
MGT – Micro Gas Turbine
LF – Load-following
CC – Cyclic-Charging
HGFR – HawkDeep Gradient Fuzzy Recurrent Control
DRPG – Deep Recurrent Policy Gradient

1. Introduction

HRES combines both wind and PV energy sources to capitalize on their complementary qualities, marking a significant breakthrough in sustainable energy integration. The wind turbines frequently reach their maximum by taking advantage of the wind speed at night or during times of low solar production. The strong wind makes the system stable, and the usage of PV panels is considered the best method for converting solar energy into power, which makes them perfect

for daytime generating. Thus, the energy capturing and delivering under varying environmental circumstances are optimized by HRES by integrating both sources via a multiport converter (Mahmoud et al. 2022). By reducing the effects of weather fluctuation, this consolidation not only improves system efficiency overall but also guarantees a steady and dependable energy supply (Samy et al. 2021). The complexity is introduced when several renewable sources are integrated using a multiport converter because synchronized control of diverse energy inputs is needed to maintain the system operating steadily and maximize power flow. Advanced control techniques are necessary for achieving these improvements (Das et al. 2021).

Furthermore, batteries are essential for maintaining grid stability, evening out irregularities, and stabilizing the DC-Bus voltage in HRES arrangements (Karthikeyan et al. 2024). Because of its comprehensive approach, HRES operates PV, wind, and other renewable energy sources in parallel with ease, making it appropriate for a variety of applications ranging from small-scale residential to large-scale industrial. HRES, which optimizes the use of renewable energy sources and limits reliance on conventional fossil fuels, is an example of a sustainable strategy to meet the world's rising energy needs while minimizing its impact on the environment (Foti et al. 2021).

A brief spike in current, known as inrush current, occurs when electrical devices are initially energized. When utilizing a multiport DC converter in HRES, inrush currents occur due to capacitive and inductive loads during system start-up or grid connection (Aljafari et al. 2023). If not adequately regulated, these currents have the potential to cause severe stress on components and compromise system stability (Rajasekaran et al. 2021). For the integrated renewable energy system, the components must operate reliably to effectively control inrush currents and provide mitigation (Xie et al. 2021).

Several machine learning algorithms, each with its own set of difficulties, have been used to handle inrush current problems in electrical systems. Based on historical data, supervised learning algorithms like SVMs and NNs have been used to forecast and manage inrush currents. However, because electrical systems are dynamic, it is difficult to get and maintain the quality and diversity of training data, which is a major factor in their effectiveness. By continuously learning and modifying control tactics in real-time, reinforcement learning approaches present intriguing possibilities (Vadivel et al. 2021). However, the massive computational resources and complex methods needed for their implementation provide scalability issues for large-scale deployment. While unsupervised learning techniques like clustering algorithms can reveal patterns of inrush currents, they didn't correctly forecast transient behaviours or adjust to changing system conditions (Heenkenda et al. 2023). In order to maximize each algorithm's unique capabilities, hybrid techniques incorporating different algorithms overcome integration challenges and guarantee reliable performance in a variety of operating scenarios in renewable energy systems (Ma et al. 2022).

In the HRES, the ramp rate describes the rate of variation in power output from renewable sources over time, such as solar or wind power. In order to preserve stability and efficiency, the multiport converter constantly modifies the power flow between sources to control this ramp rate (Nuvvula et al. 2021). Rapid variations in ramp rates, however, result in power

imbalances, which make it difficult for the converter to successfully synchronize outputs from various sources. This mismatch causes power imbalances or voltage swings in the system, which would impair the HRES's overall dependability and performance. Ramp rates in HRES have been predicted and managed using machine learning methods include LSTM networks and RNNs. These algorithms use previous data to predict power fluctuations in the future and adjust multiport converter operation accordingly. Difficulties include the computational difficulty of real-time implementation and the requirement for huge and diverse datasets for reliable forecasts (Alqahtani et al. 2024). While ensemble learning techniques such as Random Forests and Gradient Boosting provide robustness through the combination of several models, their implementation in dynamic renewable energy systems may necessitate significant computational resources and expertise (Sifakis et al. 2021). In order to overcome these obstacles, hybrid techniques that combine machine learning with conventional control strategies make use of both methodologies' advantages; nonetheless, integration and scalability continue to be crucial factors for real-world applications (Saber et al. 2021).

From the investigations, the inherent power delays in conventional converter control algorithms cause power imbalances, which lead to variations in DC Bus voltage that threaten the entire HRES, and are ineffective in predicting the occurrence of inrush current. Besides managing inrush currents, the HRES also struggles with rapid variations in load demandswhich results in over- or under-generation. Therefore, a novel solution is introduced for combining predictive and adaptive strategies to efficiently handle power imbalance between the sources.

1.1. Main contribution

To resolve these issues, a novel framework is proposed to enhance the power matching and extraction in hybrid renewable energy systems. The main contributions of this proposed method are listed below.

- To address power mismatches from inrush currents, the Intelligent Hawk Fuzzy Control Algorithm is introduced, which combines fuzzy logic with RQHO. Fuzzy logic predicts inrush currents using real-time and historical data, allowing proactive control adjustments. Thus, the RQHO optimizes the fuzzy logic, ensuring effective power matching during sudden inrush currents.
- To overcome power mismatches from ramp rate variations, the Deep Recurrent Policy Gradient technique is proposed, which combines GRU with DDPG. GRU forecasts power needs based on historical data, enabling the system to anticipate variations, while DDPG dynamically adjusts power outputs in real-time to address power imbalances from ramp rate variations, optimizing synchronization among PV panels, wind turbines, and batteries.

These contributions overcome the problems of stabilizing power output using sophisticated control techniques and optimizing synchronization among hybrid renewable sources. The paper is formatted as follows: Section 2 surveys the body of research and points out gaps; Section 3

introduces the hybrid control strategy and its operational framework; Section 4 assesses the suggested approach's performance through in-depth comparisons; and Section 5 closes with important conclusions and implications.

2. Literature survey

Jai et al. (2021) developed a Hybrid Renewable Energy Conversion System (HRECS) involving a DC/AC inverter and an AC/DC rectifier connected to a three-phase grid, incorporating PV and wind turbine generators. They introduced a novel multi-objective control approach that surpassed conventional methods by including additional control objectives, such as DC-link voltage regulation and reactive power injection into the grid, alongside PV-MPPT and optimal turbine speed regulation. A unique control strategy, based on a nonlinear model of the entire "converters-generators" system, was developed to address these objectives effectively, enhancing overall system performance. However, the research gap in this research is that while extracting maximum wind and solar energy under various conditions without direct sensors for irradiation and wind speed remaines a challenge.

Liu et al. (2022) introduced a method to optimize the control of a wind-solar storage system using power prediction to improve energy efficiency. This method predicted power using a wavelet packet neural network and independent subsystem simulation models. They combined an enhanced firefly algorithm for multi-peak scenarios with a hysteresis loop-based P&O method for single-peak MPPT. This strategy ensured dynamic tracking, speed, and optimization across both single and multiple peak scenarios. MATLAB simulations validated its effectiveness, showing superior tracking efficiency and stability compared to traditional techniques. Still, avoiding energy losses due to algorithmic restarts while maintaining reliable performance under varied environmental conditions remains a challenging research gap.

Kumar et al. (2022) introduced a method that combined a solar PV system with a doubly fed induction generator (DFIG) to optimize control algorithms for a hybrid wind-solar energy system (HWSES). They used a Grid Side Converter and Rotor Side Converter with stator flux-oriented control to manage power flow. TSR and OT algorithms were applied for wind turbines, while (MPPT) techniques, such as P&O and IC, were used for solar PV. Yet, synchronizing differential ramp rates to maintain consistent power output is an unsolved research gap.

Pangedaiah et al. (2021) suggested an HRDS that directly connected solar and wind power sources to the grid via a back-to-back voltage source converter. Solar PV modules maximized power extraction by connecting directly to the DC link without intermediate converters. A PMSG on the wind side provided reference currents for its converter using optimal torque management. This architecture enabled independent MPPT for both the energy distributed generation system and improved power transfer efficiency to the grid by converting the DC link voltage to synchronize with the grid. However, ensuring stable and reliable operation during islanding

modes, optimizing control techniques for dynamic power changes, and achieving smooth parallel operation of PMSG and PV systems for load sharing remained unresolved issues, which are considered the research gaps of this research.

Moghaddam et al. (2023) introduced an HDGS consisting of solar panels, wind turbines, and battery storage, integrated into a 33-bus imbalanced distribution network. Their method addressed a multi-objective and simultaneous problem allocation to improve PQ while reducing overall losses. PQ indices, including voltage swell, total harmonic distortion, voltage sag, and voltage unbalance, were defined. They tackled the dual challenges of creating a hybrid system and integrating it into the distribution network to minimize energy losses and enhance PQ indices. The FBS method, inspired by the swift movements of birds, was used to determine the optimal locations and sizes of HDG components. However, improving power quality indices under varying network loads and fluctuating resource generation remained a research gap.

Rosales et al. (2021) developed the Desalination Plant as a software to estimate nominal capacities for an electric-to-water micro-grid comprising a saltwater desalination system, decentralized storage, and an infinite distributed energy supply. The Desalination Plant used a global stochastic black-box approach to simulate the efficiency of the water desalination system driven by a WP plant, a PV plant, and a set of lithium-ion batteries. This approach aimed to increase the income of the renewable microgrid. Despite requiring only a few evaluations to achieve an optimal result quickly, achieving resilience and reliability with minimal computational assessments remained a major research gap in this work.

Benadli et al. (2021) presented the concept of SMC, a method for improving the efficiency of HRES that are both capable of operating on their own and in connection with the grid. With the use of the APOAM, the HRES combines PV panels, a wind turbine with a PMSG, and a battery storage system to maximize energy extraction. SMC was put into place to effectively maximize wind energy conversion and control PV voltage. However, adapting SMC to various weather conditions and load types is considered a challenging research gap.

Bashar et al. (2021) introduced a hybrid energy system aimed at meeting both thermal and electrical demands in an off-grid network. The system integrated Li-ion batteries, an MGT, wind turbines, and solar PV, with performance analyzed using HOMER software, and compared CC and LF dispatch strategies. The CC strategy demonstrated significant benefits, including reduced hardware size, lower costs, decreased CO_2 emissions, and a higher renewable energy fraction. By optimizing power management and waste heat recovery, the CC approach enhanced system efficiency and environmental impact. The LF strategy, while meeting only electrical loads, resulted in substantial excess energy generation. However, reliance on waste heat recovery for thermal load during low operational periods of the MGT is a challenging research gap.

Singh et al. (2024) developed an optimum power forecasting technique for hybrid renewable energy systems integrating photovoltaic, wind, and solar plants. The approach combined historical atmospheric and power generation data with preprocessing steps to minimize noise and improve input quality. To enhance deep learning model efficiency, K-Means clustering was employed to optimize training periods and identify representative data groups. A hybrid recurrent neural network based on GRUs was implemented for forecasting, outperforming traditional

models in terms of accuracy and error reduction. The proposed technique achieved superior accuracy for large-scale power forecasting and demonstrated resilience against variability in renewable clusters. Still, the model's dependence on high-quality atmospheric data and extensive preprocessing restricts real-time deployment in resource-limited microgrid environments, indicating a direction for future optimization.

Paulsamy et al. (2025) introduced a grid-tied hybrid renewable energy system integrating photovoltaic, wind energy conversion systems WECS, and battery storage, with a focus on efficient power conversion and energy management. A Re-lift Luo converter was employed to enhance PV voltage gain, reduce ripple, and mitigate parasitic effects, thereby improving grid synchronization performance. Simulation in MATLAB/Simulink and real-time prototype validation demonstrated high efficiency, a 1:10 voltage gain, reduced oscillations, and an efficient Total Harmonic Distortion, highlighting superior power quality. Nevertheless, the system's reliance on computationally intensive hybrid optimization and neural network models limits scalability for real-time applications in low-resource environments.

From the above analysis, it is determined that Jai et al. (2021) faced challenges in extracting maximum wind and solar energy without direct sensors, and Liu et al. (2022) struggled with avoiding energy losses and maintaining reliability under varied conditions. Kumar et al. (2022) had difficulties synchronizing ramp rates for consistent power output, and Pangedaiah et al. (2021) encountered issues with stable operation during islanding and dynamic power changes. Moghaddam et al. (2023) faced challenges in maintaining power quality under fluctuating loads. Rosales et al. (2021) had difficulty achieving resilience and reliability with minimal computational evaluations, and Benadli et al. (2021) struggled with adapting SMC to diverse weather conditions. Bashar et al. (2021) faced challenges with waste heat recovery during low operational periods, Singh et al (2024) struggled with the model's dependence on high-quality atmospheric data and extensive preprocessing, and Paulsamy et al. (2025) had difficulties with the system's reliance on computationally intensive hybrid optimization. Therefore, an efficient method is needed to resolve power imbalances and mismatches in ramp rates.

3. Proposed methodology for handling power mismatches and optimizing power extraction in Hybrid Renewable Energy Systems (HRES)

In HRES systems, resolving power imbalances and mismatches in ramp rates is essential to preserving system stability and efficiency. Hence, a novel HGFR is proposed by combining two approaches to optimize power extraction and stabilize system performance in HRES by managing inrush currents and ramp rate mismatches efficiently. Immediate power matching is challenging due to the inherent response delays in converter control algorithms, which take time

to sense, process, and adjust. This delay causes a power imbalance between supply and demand, leading to variations in DC-Bus voltage that threaten the stability of the entire hybrid renewable energy system. Most current control algorithms are reactive, addressing issues only after an inrush current occurs, rather than predicting and pre-emptively adjusting for anticipated surges. Hence, to address power mismatches from inrush currents, a novel Intelligent Hawk Fuzzy Control Algorithm is introduced by using fuzzy logic to predict and manage these surges. It utilizes historical and real-time data for proactive adjustments, providing a flexible and adaptive control framework that handles uncertainties and nonlinearities in renewable energy sources. Inspired by the hunting habits of Harris hawks, the RQHO algorithm incorporates quasi-reflection that enhances the optimization of control parameters (by minimizin a cost function combining DC-bus voltage deviation, power mismatch, and transient settling time) by refining the predictive capabilities provided by the fuzzy logic.

This combination of fuzzy logic and RQHO enhances both the exploration and exploitation phases, optimizing control parameters more effectively and ensuring that the control system quickly converges to optimal solutions. The criterion of this optimization is to minimize a multi-objective cost function that penalizes DC-link voltage deviations, power mismatch, and settling time. This integrated approach maintains power balance even in the face of sudden inrush currents.

In addition to managing inrush currents, hybrid renewable energy systems also face challenges with rapid variations in load demands, which lead to over- or under-generation. Traditional control algorithms, which rely on predefined rules or linear techniques, often suffer from slow responses and inadequate synchronization among power sources, rendering them ineffective in handling ramp-rate mismatches. Hence, to address these issues DRPG technique is proposed by combining DDPG for real-time adjustments with GRU for accurate power forecasting. Together, accurate forecasts are produced by GRUs, and optimal decision-making is made easier by DDPG in real-time. This improves synchronization between PV panels, wind turbines, and batteries, effectively reduces transient power imbalances, stabilizes DC bus voltage, and boosts overall system dependability and efficiency.

The architecture of the proposed technique is shown in Figure 1. The load demand is first applied to the grid and subsequently to a transformer, a filter component filters the AC signal, which is then transformed to DC via an AC/DC converter and sent over a DC bus to the multiport DC converter. In order to achieve the best possible power management, the suggested approach presents the HGFR Control algorithm, which combines Intelligent Hawk Fuzzy Control with DRPG approaches. The DRPG manages power imbalances and ramp rate mismatches by using GRUs and DDPG. The wind turbine output is then controlled by the gearbox and PMSG, and the system routes DC energy from batteries and PV panels to the multiport DC converter. To make sure that the modified power effectively meets the load demand, this procedure is then reversed.

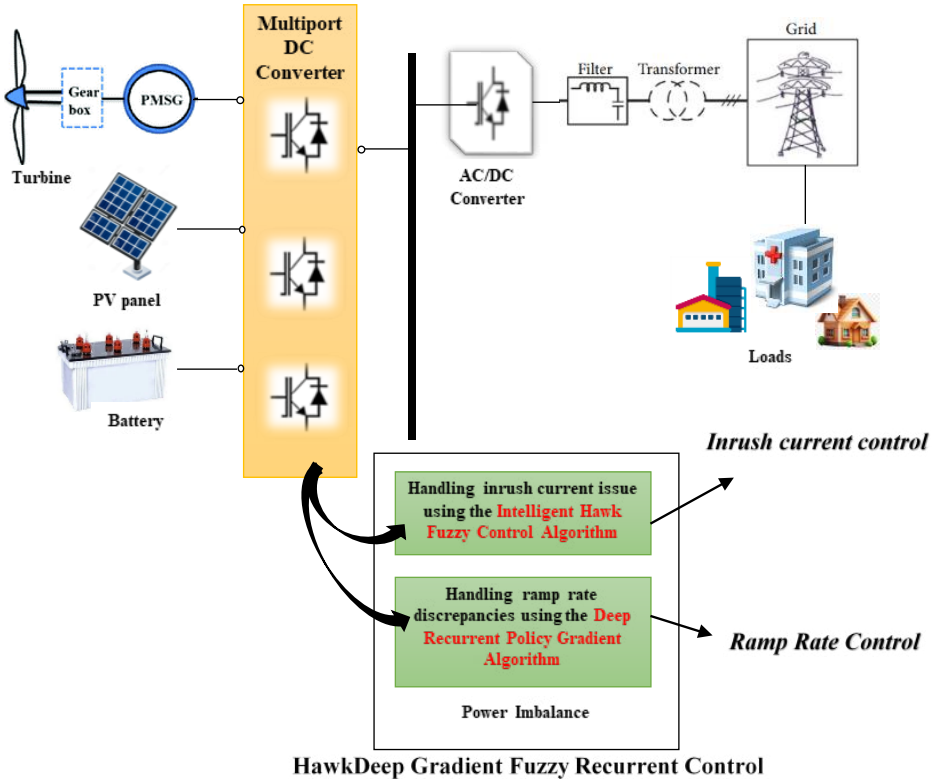

Fig. 1. Overall architecture of the proposed model

Rys. 1. Ogólna architektura proponowanego modelu

3.1. Intelligent Hawk Fuzzy Control Algorithm

The Intelligent Hawk Fuzzy Control Algorithm is proposed to overcome ramp rate mismatches and inrush current management issues in HRES. By evaluating previous and current data, this approach uses fuzzy logic to anticipate and control unexpected spikes in power, allowing for proactive rather than reactive adjustments. It successfully manages the uncertainties and nonlinearities of renewable energy sources by modeling human decision-making. This method guarantees more precise predictions and optimal control when combined with the RQHO algorithm, which minimizes a cost function that combines DC-bus voltage deviation, power mismatch, and transient settling time control parameters via quasi-reflection techniques inspired by Harris hawk hunting strategies. When combined, these strategies increase system efficiency and stability by preserving power balance even in the face of sudden variations in load demands and power generation.

The algorithm is initialized by the control system, continuously monitoring real-time data from various renewable energy sources, such as PV panels, wind turbines, and batteries, as well as the load demands. This data is then subjected to fuzzy conversion, where numerical values are transformed into fuzzy sets representing linguistic variables such as “low”, “medium”, and “high” inrush current risks. After processing, fuzzy rules are applied to the data. These guidelines are used to direct decisions: if a medium inrush current is detected with a high load demand, the switching frequency is increased; if a strong inrush current is detected with a low battery charge, the power output is reduced; and if the inrush current is moderate, the current system configurations are maintained. It transforms the fuzzy output from all of the rules into a crisp control action using Equation (1) after aggregating the result from each rule (Parvaneh and Khorasani 2020).

$$Crisp_{(t)} = \frac{\sum_{i=1}^{j} Out_i \times Member_{Degree_i}}{\sum_{i=1}^{j} Member_{Degree_i}} \tag{1}$$

At time *t*, the last crisp control action is represented by $Crisp_{(t)}$. This value is obtained by adding together the fuzzy rule outputs and taking into consideration the membership degrees of each rule is represented by $Member_{Degree_i}$. The output value corresponding to the *i*-th fuzzy rule is indicated by and is determined by the conditions of that rule. $Member_{Degree_i}$, which ranges from 0 to 1, represents the membership degree for the *i*-th fuzzy rule. The total number of fuzzy rules evaluated is denoted by *j*.

By using this method, inrush current is proactively managed, which makes the hybrid renewable energy system operate more steadily and effectively. After that, the control strategy is further refined using the RQHO approach. The RQHO algorithm is incorporated into the control system to optimize the fuzzy logic parameters, drawing inspiration from the hunting behavior of Harris hawks. Quasi-reflection methods are incorporated into RQHO to improve the phases of exploration and exploitation. With the help of the quasi-reflective mechanism, the algorithm can dynamically modify its search approach, avoiding local optima and accelerating its convergence to global optimal solutions. Three crucial steps are involved in initializing the algorithm to optimize the fuzzy controller’s output: exploration, transition from exploration to exploitation and exploitation (Rizwan et al. 2021).

Exploration phase

The RQHO algorithm simulates Harris hawks, which randomly sit at different spots in order to find optimal solutions during the exploration phase. With an equal chance (ϵ), every hawk uses one of two tactics: it either stays close to other hawks to take advantage of group exploration or it searches for new spots on its own.

When $\epsilon < 0.5$, hawks utilize other solution’s positions using Equation (2):

$$Pos_{(t)} = Pos_{b(t)} - Pos_{avgloc(t)} - rand_1\left[L_{limit} + rand_2\left(U_{limit} - L_{limit}\right)\right] \tag{2}$$

Where, the best hawk's position at time t is represented by $Pos_{b(t)}$. The average location of every position in the population at that particular time is indicated by $Pos_{avgloc(t)}$. The parameter space's lower and upper limits are defined, respectively, by the parameters L_{limit} and U_{limit}. Furthermore, the random variables $rand_1$ and $rand_2$ in the interval [0,1] are employed to modify the algorithm's exploration and exploitation tactics.

When $\epsilon < 0.5$, hawks use random tall trees using Equation (3):

$$Pos_{(t+1)} = Pos_{b(t)} - rand_3 \left| Pos_{r(t)} - 2 \cdot rand_4 \cdot Pos_{(t)} \right| \tag{3}$$

where:

$Pos_{r(t)}$ – randomly chosen locations from the current population,
$Pos_{(t)}$ – the posititon vector of the hawk,
$Pos_{(t+1)}$ – the position vectors of solutions at $t + 1$ iterations,
$Pos_{b(t)}$ – the best hawk's position at time.

Transferal from exploration to exploitation

In the transfer from exploration to exploitation, RQHO algorithm transitions from randomly perching to focusing on regions identified as promising during exploration. The hawks now concentrate their search around these optimal areas, using the quasi-reflection mechanism of RQHO to refine control parameters using Equation (4).

$$Energy_{cs} = 2 \cdot Energy_{initial} \cdot \left(1 - \frac{t_{current}}{t_{total}} \right) \tag{4}$$

where:

$t_{current}$ – the current iteration,
t_{total} – the total number of iterations,
$Energy_{initial}$ and $Energy_{cs}$ – the initial and current escape energies, randomly selected values within the range of [−1,1]. $Energy_{initial}$ randomly changes inside the interval [−1,1] at each iteration.

Exploitation phase

In this phase, the algorithm refines its search by focusing on promising solutions identified during exploration. The position vector $Pos_{(t)}$ of the current solution is updated to $Pos_{(t+1)}$ using the Formula (5):

$$Pos_{(t+1)} = \Delta Pos_{(t)} - Energy_{cs} \left| J_{esc} \cdot Pos_{b(t)} - Pos_{(t)} \right| \tag{5}$$

$Pos_{(t)}$ represents the current solution's position vector, $Pos_{(t+1)}$ represents its updated position vector for the following iteration, $Energy_{cs}$ is the current escape energy at iteration and J_{esc} is the random escape power. The best solution identified thus far is represented by the position vector

$Pos_{b(t)}$. $Pos_{b(t)} - Pos_{(t)}$ is the difference vector between the best location and the current position and J refers to the random escape power, calculated as using the Equation (6) below:

$$J_{esc} = 2\left(1 - rand_5\right) \tag{6}$$

where:

J_{esc} – represents the random escape power and it is a number chosen at random from the interval [0,1],

$rand_5$ – represents the random variable.

To further improve the optimization process, the Quasi-Reflexive is used after the exploitation phase, which narrows the search around the best options. The Quasi-Reflexive process creates new candidate solutions in order to add variety and prevent local optima. New candidate solutions are produced by the quasi-reflection process using the following Formula (7):

$$X^{qr} = rand\left(\frac{L_{limit} + U_{limit}}{2}, S\right) \tag{7}$$

where:

X^{qr} – represents the candidate solution generated by quasi-reflection, a random number from a uniform distribution in the range $\frac{L_{limit} + U_{limit}}{2}$ and S is generated by $rand\left(\frac{L_{limit} + U_{limit}}{2}, S\right)$. This process is carried out in D dimensions for every parameter in solution S. L_{limit} and U_{limit} stand for lower and upper bounds, respectively. The algorithm's exploration capabilities are improved by combining the quasi-reflection technique with the Harris Hawks Optimizer; this ensures a more exhaustive search of the solution space and raises the fuzzy logic control system's overall performance for HRES.

The control system adjusts to HRES dynamically as the RQHO algorithm optimizes fuzzy logic settings, even in the event of unexpected surges. This integration guarantees quick convergence to the best options, balancing the supply and demand of electricity. The control system, which runs continuously, monitors system performance and modifies the converter duty cycle and control parameters in real time to preserve efficiency and stability. It adjusts to changing circumstances and ensures dependable and steady power management in the face of unpredictable and variable issues by utilizing real-time data and past trends.

Figure 2 illustrates the architecture of the proposed integration. Data Collection collects historical and real-time data from multiple sources. This data is fuzzified, which turns numerical inputs into fuzzy values. Then, the Fuzzy Inference System applies predefined fuzzy rules to these values to produce fuzzy outputs. RQHO is used to optimize control parameters, refining these

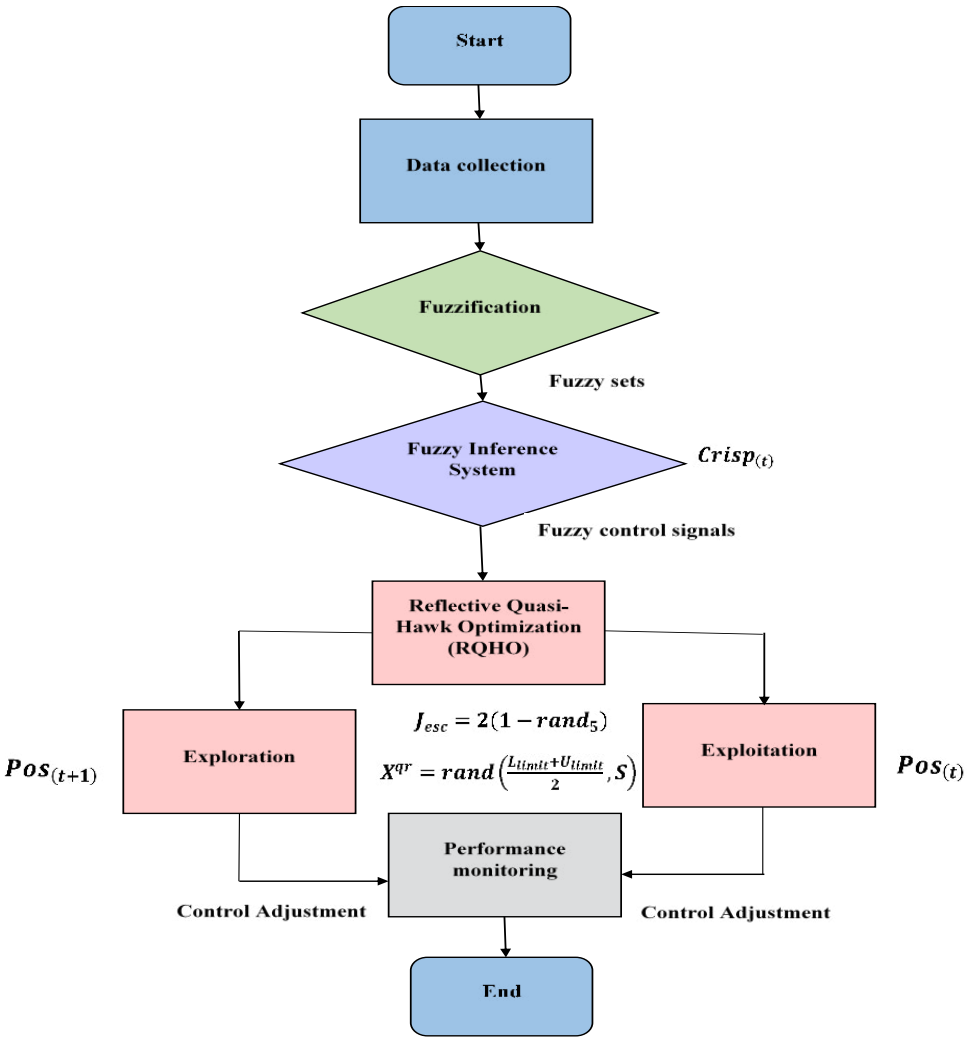

Fig. 2. Flowchart of the Intelligent Hawk Fuzzy Control Algorithm

Rys. 3. Schemat blokowy inteligentnego algorytmu sterowania rozmytego typu Hawk

parameters through phases of exploration and exploitation. The optimized control actions are integrated with the fuzzy outputs in the Integration stage, leading to Control Adjustment to fine-tune the system's performance. System Performance Monitoring verifies that the adjustments improve stability and efficiency. DRPG manages differences in ramp rates that is explained in section 3.2.

3.2. Deep Recurrent Policy Gradient

The DRPG system handles ramp rate discrepancies while addressing slow reactions and insufficient synchronization between power sources. Using DDPG and GRU networks, it combines time-series prediction with real-time control. The GRU is first trained on historical data in order to create the first prediction models. The system continuously gathers real-time data from several power sources and load needs. By examining temporal data patterns, the GRU network forecasts short-term power generation and load fluctuations (Huang et al. 2023), which is explained using the equations below.

The input of the update gate is computed as below using the following Equation (8),

$$af_{up}^{t} = \sum_{i=1}^{Input} w_{if} x_{infe}^{t} + \sum_{h=1}^{hidden} w_{hs} G_{hidden}^{t-1} \tag{8}$$

where:

$hidden$ – the number of hidden units at time t–1,
$Input$ – the number of input features,
af_{up}^{t} – represents the update gate input for GRU at time (t),
G_{hidden}^{t-1} – the output of the hidden neuron(s) at the previous time step (t – 1),
up – the number of update gate vectors,
x_{infe}^{t} – the i_{th} is the input feature value at time step t,
w_{if} – the weights for the input features,
w_{hs} – the weights for the hidden state from the previous time step.

This helps to blend new data with historical data by determining how much of the new information should be included into the concealed state. After that, this input is converted in the update gate using Equation (9),

$$G_{up}^{t} = f\left(af_{up}^{t}\right) \tag{9}$$

where:

the update gate at time t, G_{up}^{t} is the updated hidden state at time t, which is computed by applying the activation function f to the update gate input af_{up}^{t}. By striking a balance between maintaining the existing hidden state and integrating fresh input data, this gate decides how much of the new information is included in the hidden state.

To determine how much of the prior state to forget, the reset gate input is calculated using a sigmoid function to ascertain retention levels. The candidate hidden state is then computed using a tanh function after the reset gate has changed the candidate hidden state input. In order to improve the model's predictions, the candidate state and the prior state are combined based on the update gate to update the hidden state, which is explained below using Equations from (10) to (14):

$$a_{rg}^{t} = \sum_{i=1}^{input} w_{i_{reset}} x_{infe}^{t} + \sum_{h=1}^{hidden} w_{h_{reset}} G_{hidden}^{t-1} \tag{10}$$

$$G_{rg}^{t} = f\left(af_{rg}^{t}\right) \tag{11}$$

$$a_{h'}^{\sim t} = G_{up}^{t} \sum_{h=1}^{hidden} w_{h_{h'}} G_{h}^{t-1} + \sum_{i=1}^{input} w_{i_{h'}} x_{infe}^{t} \tag{12}$$

$$G_{h'}^{\sim t} = \varnothing\left(a_{h'}^{\sim t}\right) \tag{13}$$

$$G_{h}^{t} = \left(1 - G_{up}^{t}\right) G_{h'}^{\sim t} + G_{up}^{t} G_{h}^{t-1} \tag{14}$$

where:

rg – the number of reset gate vectors,
a_{rg}^{t} – the reset gate input at time (t),
$a_{h'}^{\sim t}$ – the candidate hidden state input,
af_{rg}^{t} – the pre-activation value before applying the non-linearity,
$w_{i_{reset}}$ and $w_{h_{reset}}$ – the weights for the reset gate,
G_{rg}^{t} – the output activation of the rg-unit
h' – the number of hidden vectors at time step t,
$w_{hh'}$ and $w_{ih'}$ – the candidate hidden state weights,
$\varnothing$ – non-linear activation function to the candidate input $a_{h'}^{\sim t}$ and the hidden state G_{h}^{t} is calculated by blending the candidate hidden state $G_{h'}^{\sim t}$ with the previous hidden state G_{h}^{t-1} using the update gate G_{up}^{t}.

The power output from each source is continuously adjusted by the DDPG algorithm based on the predictions made by the GRU network. By experimenting with various power output configurations and monitoring the ensuing system states, the DDPG network communicates with the multiport DC converter system. The following actions are taken in order to maximize this (Xia and Wang 2024).

Equation (15) is used for gradient estimation:

$$\nabla_{\theta_\mu} J \approx E_{st_t \sim \rho, ac_t \sim \mu}\left[\nabla_{\theta_\mu} \mu\left(st_t; \theta_\mu\right) \nabla_{ac} M\left(st, ac \mid \theta_M\right)|_{st=st_t, ac=\mu(s_{tt})}\right]\mu \tag{15}$$

The goal of the Critic network is to reduce the value function's loss function $L(\theta_M)$, which quantifies the difference between the function's predicted value and the target value. $\nabla_{\theta_\mu} J$ represents gradient of the expected return J with respect to the actor's parameters θ_μ is the parameters of the actor network μ, $E_{st_t \sim \rho, ac_t \sim \mu}$ represents the expection taken over in which

the st_t~ρ states the sample from the state distribution and $\mu(s_{tt})$ represents the policy function. Among them, the Critic network's target value Y_j has been changed to:

$$Y_j = re_j + \gamma_{dis} M'\left(s_{tj+1}, \mu'\left(st_{j+1} \mid \theta_{\mu'}\right)\theta_{M'}\right) \tag{16}$$

The target value is computed using the following Equation (17):

$$L\left(\theta_M\right) = \frac{1}{N_{bs}} \sum_j \left(M\left(st_j, ac_j \mid \theta_M\right) - Y_j\right)^2 \tag{17}$$

The Critic network's specifications is modified using the Equation (18) below:

$$\theta_M \leftarrow \theta_M - \alpha_1 \nabla_{\theta_M} L\left(\theta_M\right) \tag{18}$$

where:

the variables are state st_j, action ac_j, and reward re_j. The discount factor, represented by γ_{dis}, is utilized to determine the significance of future benefits. The value function, denoted by (st, $ac|\theta_M$), is utilized to assess the worth of a state st and action ac, with θ_M serving as the parameter. The policy function, $\mu(s_{tt})$, is utilized to create actions in a specified state. The parameter of the policy function is represented by θ_μ. The parameter update step size is controlled by the learning rate, denoted by α_1. The batch size at each update is indicated by N_{bs}.

The DDPG algorithm makes real-time power output adjustments based on these predictions, experimenting with various setups and fine-tuning its control policies in response to feedback. This procedure keeps the DC bus voltage steady, synchronizes the power sources, and adjusts to the environment. In addition to reducing power imbalances, the continuous feedback loop of data collecting, prediction, adjustment, and learning also increases system dependability and efficiency.

Figure 3 illustrates the integration of GRU and DDPG to optimize control in hybrid renewable energy systems. Initially, historical and real-time data are collected from renewable sources and load demands. This data is processed by the GRU, which generates forecasts of future states and demand patterns. These forecasts are then fed into the DDPG framework, where the Actor network determines the optimal actions based on the predicted states, while the Critic network evaluates these actions. The DDPG adjusts control parameters and provides feedback to refine the policy. The integrated system combines these forecasts and control actions to enhance stability and efficiency, resulting in improved synchronization, reduced power imbalances, and stable DC bus voltage.

Overall, the efficient and dependable operation of the HRES is guaranteed by the Intelligent Hawk Fuzzy Control Algorithm and DRPG, which effectively reduce power imbalances and maintain a steady DC bus voltage. These strategies improve overall system performance and stability, adjusting to changing circumstances and enhancing long-term reliability by utilizing sophisticated control and optimization approaches.

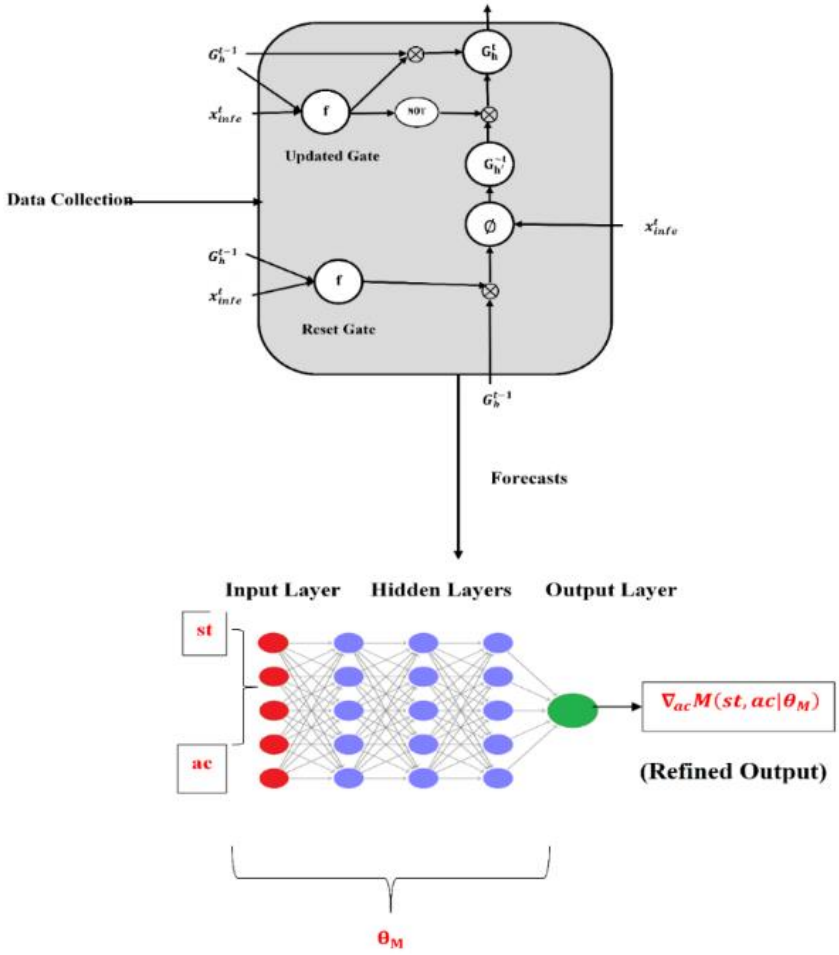

Fig. 3. Architecture of the DRPG

Rys. 3. Architektura DRPG

4. Result and discussion

This section provides a detailed analysis of the HGFR Control system's performance and implementation discoveries. A comparative analysis is also provided to show how well the suggested method works in HRES to optimize power extraction and stabilize system performance while efficiently managing inrush currents and ramp rate mismatches. The simulation tools and their configurations are represented in Table 2. The proposed approach is simulated using

MATLAB, and the assessments are carried out by adjusting the load circumstances and system characteristics.

Table 2. System configurations

Tabela 2. Konfiguracje systemu

Software	MATLAB
OS	Windows 10 (64-bit)
Processor	Intel i5
RAM	8GB RAM

4.1. Simulated output of the proposed model

This section explains the simulated output of the suggested model for improving power extraction and matching in hybrid renewable energy systems using HawkDeep Gradient Fuzzy Recurrent Control.

Figure 4 (a) shows the performance of the simulated control voltage bus, the voltage ranges between 0 V and 1 V. At the initial instant ($t = 0$ s), the voltage begins at 0 V. Almost immediately, within a fraction of a second, the voltage rises sharply to its maximum level of approximately 1 V. From this point onward, throughout the entire interval from 0.1 s to 3 s, the voltage remains constant and stabilized at 1 V, with no observable fluctuations or drops. This flat response indicates that once the system reaches its steady-state operating voltage, it maintains a consistent level across the entire observed time window. Thus, the figure 4 (b) depicts the RMS value error over time, and the error first increases to a maximum, then declines sharply before stabilizing at a particular point, which is the range between 15 and 25 with a variation of 2 s. It reflects the system's adjustment phase, where the algorithm fine-tunes its parameters.

Moroever Figure 4 (c) illustrates the Multiport Output Voltage simulation for the proposed method. It demonstrates gradual changes in the output voltage, which is approximately 290 V over time, starting with a noticeable drop and then varying little around a steady level of 0 V within 5 s. Furthermore, Figure 4 (d) illustrates the DC voltage simulation for the proposed method. The graph demonstrates the DC voltage rising at first and then falling significantly. After that, there aren't many changes in the voltage as it steadily stabilizes and eventually reaches a constant state with just minor fluctuations. This significant demonstrates that the system's efficient maintenance of voltage stability by highlighting the efficacy of the Intelligent Hawk Fuzzy Control Algorithm in conjunction with Reflective Quasi-Hawk Optimization for managing and stabilizing DC voltage.

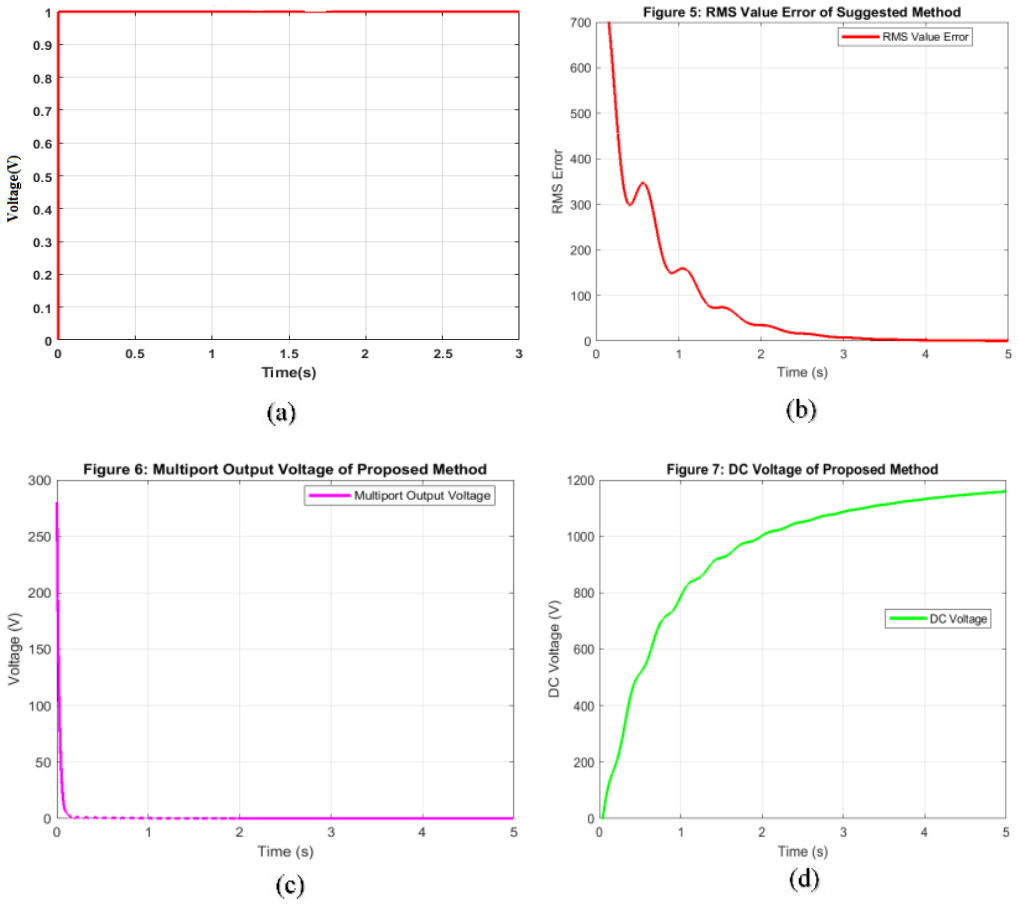

Fig. 4. (a) Control Voltage Pulse of the proposed model, (b) RMS Value Error of the suggested method, (c) Multiport Output Voltage of the suggested model and (d) DC voltage of the proposed model

Rys. 4. (a) Impuls napięcia sterującego proponowanego modelu, (b) Błąd wartości skutecznej sugerowanej metody, (c) Napięcie wyjściowe wieloportowe sugerowanego modelu oraz (d) Napięcie prądu stałego proponowanego modelu

Figure 5 (a) depicts the ramp rate simulation for the proposed method. The graph exhibits a notable drop along the time axis after a first strong decline. After that, there is a noticeable decline and a string of oscillations of differing sizes until things finally stabilize. Moroever Figure 5 (b) illustrates how the suggested model's injected voltage behaviour changes over time. The graph first exhibits notable oscillations between –300 and 300, indicating a high degree of volatility. After that, there are discernible decline patterns and a sequence of oscillations with different intensities. The system eventually moves to a less fluctuating, more stable condition. These results demonstrate the adaptability of the system in abrupt changes in ramp rate, and how well the suggested approach handles sudden voltage changes highlights the benefits of both

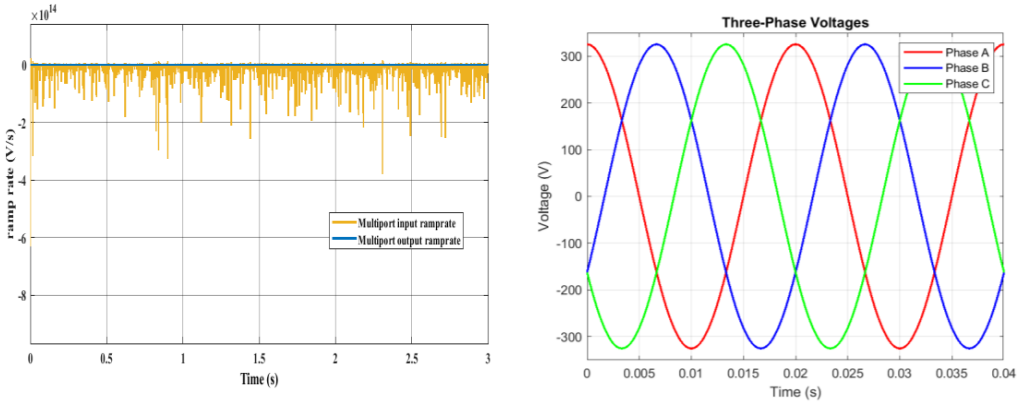

(a) (b)

Fig. 5. (a) Ramp Rate of the proposed model and (b) Injected Voltage of the proposed model

Rys. 5. (a) Współczynnik narastania proponowanego modelu oraz (b) Napięcie wtryskiwane proponowanego modelu

Reflective Quasi-Hawk Optimization and the Intelligent Hawk Fuzzy Control Algorithm for preserving stability in dynamic environments.

Figure 6 illustrates the load current and source intermediate behavior of the proposed model across the three-phase grid (Phase A, Phase B, and Phase C). Initially, the plots show significant peaks, valleys, and large oscillations, reflecting transient responses under abrupt power changes. The oscillations gradually reduce over time, and the system reaches a stable state. This demonstrates the effectiveness of the integrated HGFR control framework comprising the DRPG, Reflective Quasi-Hawk Optimization, and Intelligent Hawk Fuzzy Control Algorithm in stabilizing the three-phase system and ensuring reliable operation under dynamic conditions.

4.2. Performance of the proposed model

This section examines the experimental outcomes of the suggested HRES optimization strategy. Power imbalances and ramp rate mismatches are efficiently managed by the integrated technique, which combines the RQHO and Intelligent Hawk Fuzzy Control Algorithm. The outcomes show that the approach can guarantee HRES operates steadily and effectively.

The three-phase load current and source intermediate behavior of the proposed method are represented in Figure 7 (a). Initially, notable oscillations and peaks are observed across all three phases, reflecting transient behavior during power mismatch events. Over time, the system transitions to a more stable operating state with reduced oscillations. Thus, the convergence curve of the proposed method is represented in Figure 7 (b). As the algorithm advances, the curve shows a severe initial decrease that is followed by a quick gain in performance. Subsequently,

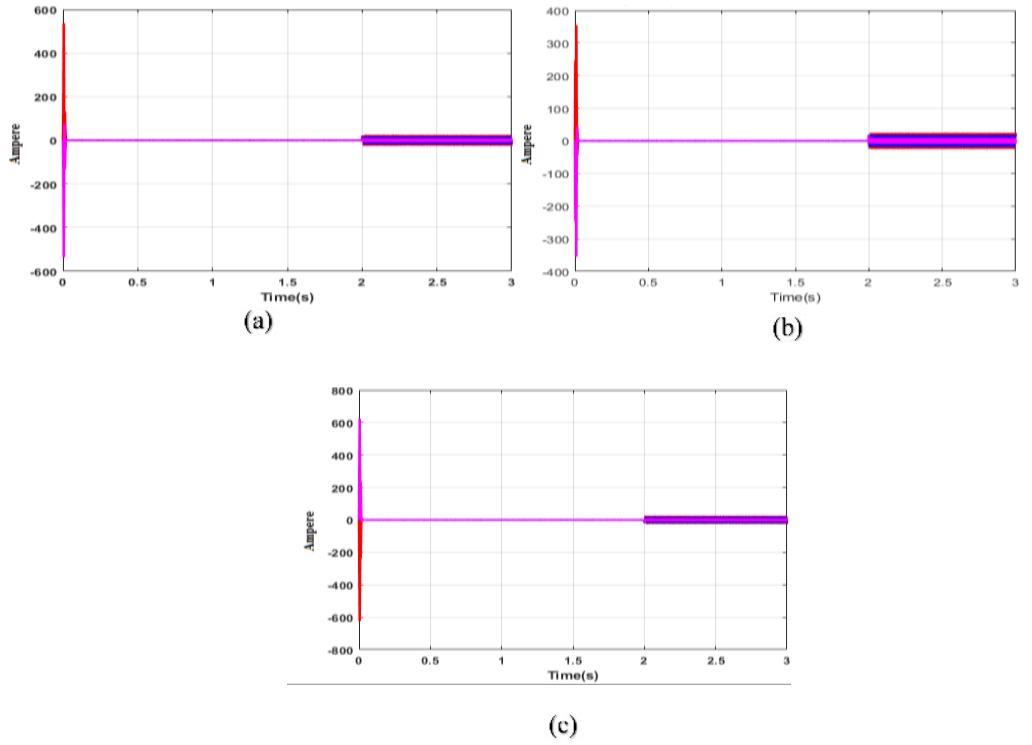

Fig. 6. Load current and Source Intermediate of the proposed model: (a) Phase 1, (b) Phase 2, (c) Phase 3

Rys. 6. Prąd obciążenia i źródło pośrednie proponowanego modelu: (a) Faza 1, (b) Faza 2, (c) Faza 3

it attains stability at a constant value, signifying that the technique successfully approaches a steady performance threshold.

Moroever, Figure 7 (c) shows MAPE for the suggested method during the training period. The model's learning and adaptation process during training is reflected in this pattern. Furthermore, the forecasting load of the suggested model during the training phase is shown in Figure 7 (d). The graph displays an initial climb, a slight decrease, a significant surge, and then volatility. These results show how the model adapts during training, the capability of the integrated HGFR framework, and maintain reliable power delivery at the rated output of 72.1 kW. The model's forecasting accuracy and stability are effectively increased by integrating the Intelligent Hawk Fuzzy Control Algorithm with the DRPG method, which incorporates GRU and DDPG. This leads to improved performance and reliability over time.

The accuracy, precision, recall, and F1-score analysis of the proposed method is shown in Figure 8, and the proposed model performs well in several operational circumstances. It achieves an accuracy of 0.98 after 6 epochs, and the variance in accuracy demonstrates the system's skills in adjusting to shifting circumstances and handling power imbalances and ramp rate mismatches. This system achieves the precision of 0.92 after 6 epochs, indicating its strong performance

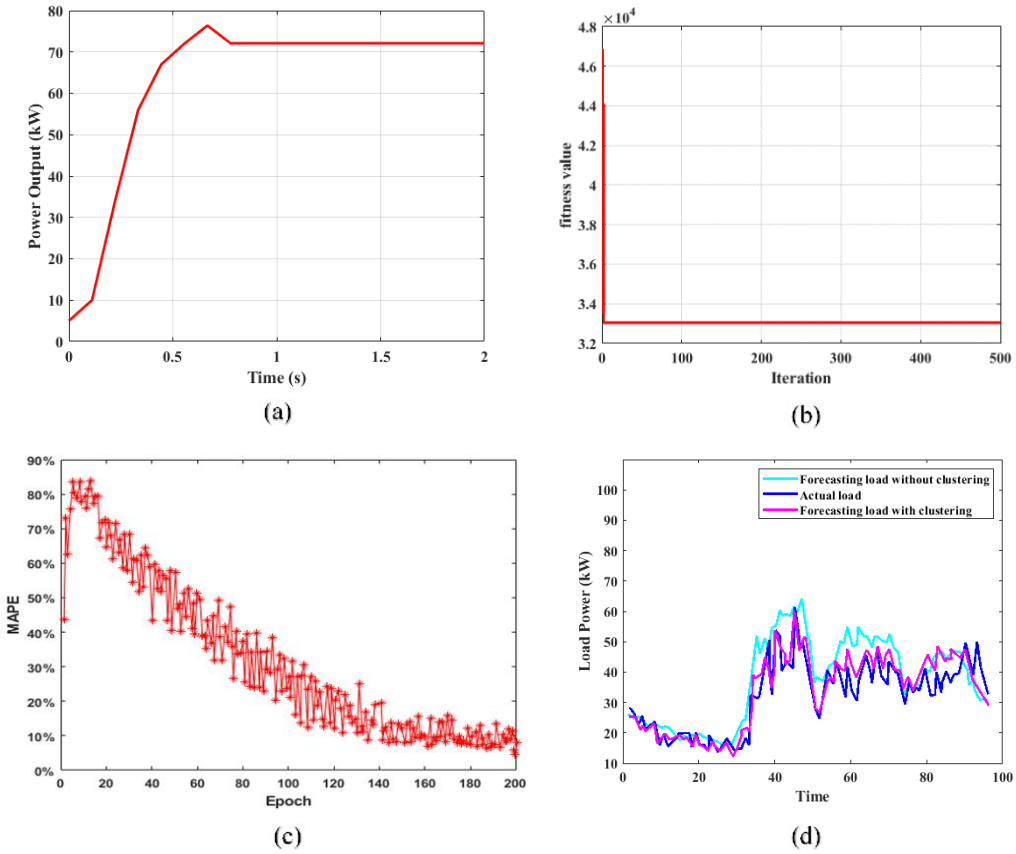

Fig. 7. (a) Power Output, (b) Convergence Curve, (c) Mean Absolute Percentage Error (MAPE) and (d) Forecasting Load of the proposed model

Rys. 7. (a) Moc wyjściowa, (b) Krzywa zbieżności, (c) Średni bezwzględny błąd procentowy (MAPE) oraz (d) Obciążenie prognozowania proponowanego modelu

throughout a range of operational situations. This variance in accuracy demonstrates the system's ability to reliably generate precise forecasts while controlling power imbalances and ramp rate mismatches.

Moroever the system's ability to detect pertinent instances across a range of operational circumstances is demonstrated by a recall of 0.94 after 6 epochs, and its range highlights the system's capacity to precisely identify and react to noteworthy occurrences while adjusting for power imbalances and ramp rate mismatches. Furthermore, the system's balanced performance across various operational circumstances is reflected in its F1-score of 0.91 after the 6 epochs, and this range shows how well the system manages power imbalances and ramp rate mismatches while striking a fair balance between recall and precision. These results show how well the GRU model can adapt in real time to a variety of inputs and maintain steady, effective operation of HRES.

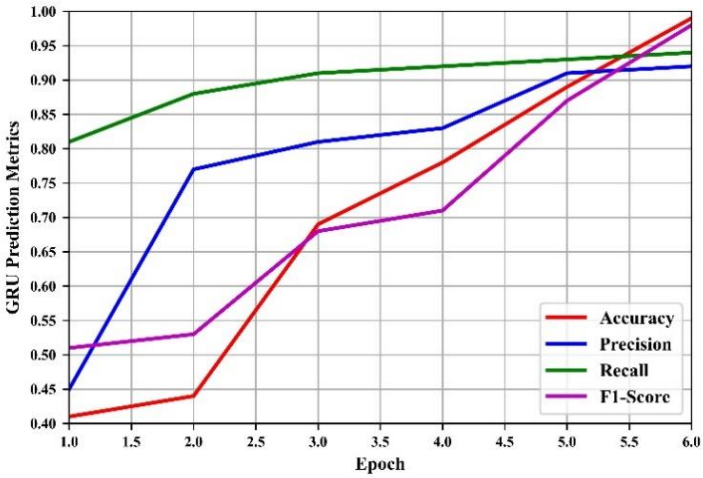

Fig. 8. Accuracy, Precision, Recall and F1-score of the proposed model

Rys. 8. Dokładność, precyzja, przypomnienie i wynik F1 proponowanego modelu

Figure 9 shows the proposed model's voltage-current (V-I) and voltage-power (V-P). The V-I curve displays a large current at low voltages that stabilises at the maximum power point (MPP) and then declines as voltage increases. At the MPP, the V-P curve peaks and then starts to decline. The power surges are efficiently managed by the Intelligent Hawk Fuzzy Control Algorithm in conjunction with RQHO. Ramp rate mismatches are addressed and DC bus voltage is stabilised by DRPG technique, which combines GRU with DDPG. This progression highlights

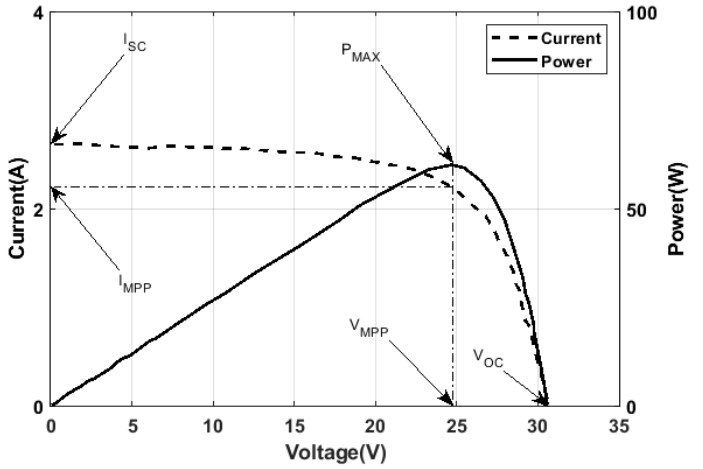

Figu. 9. Voltage-current and voltage-power of the proposed model

Rys. 9. Napięcie-prąd i napięcie-moc proponowanego modelu

the maximum power points occurring within the 25–27 V range across the different curves and the system's response to these variations is optimized by the Intelligent Hawk Fuzzy Control Algorithm in conjunction with RQHO.

4.3. Comparative analysis of the proposed method

This section provides a thorough discussion of the recommended technique's efficacy as well as the results attained. The following metrics are used for comparison: voltage output, voltage variation, power variation, power output, statistical error, efficiency, standard deviation, response error, area under control, and frequency deviation.

The voltage output performance of the suggested approach is shown in Figure 10 (a) in comparison to the methods that are currently in use, such as PSO-GA, P2O, and INC (Parvaneh and Khorasani 2020). The proposed approach outperforms the current techniques, achieving a voltage output of 2 V. PSO-GA attains a voltage output of 1.20 V, P&O reaches 1.88 V, and INC reaches 0.30 V. In particular, this shows the suggested strategies' performance in producing a higher voltage output. Thus, the proposed method's voltage variation differs from PSO-GA, P_2O, and INC (Parvaneh and Khorasani 2020). The graph shows that, in comparison to the current methods, the suggested method achieves a voltage variation of 0.15s, which is noticeably larger. In particular, P&O displays a variation of 0.54 s, INC shows a variation of 0.30 s, and PSO-GA shows a variation of 0.2 s.

Moroever the power variation of the suggested strategy is shown in Figure 10 (b). The graph demonstrates the suggested approach outperforms the current methods, achieving a power variation of 96.03 kW. In particular, 1.20 kW of variance is shown by PSO-GA, 1.88 kW by P&O, and 0.30 kW by INC (Parvaneh and Khorasani 2020). Furthermore, the proposed method's power output is demonstrated, and it outperforms the existing methods, achieving a power output of 72.1 kW. PSO-GA produces 58.64 kW of power; P&O produces 53.68 kW; and INC produces 56.29 kW (Parvaneh and Khorasani 2020). This improved performance demonstrates how well the sophisticated procedures used in the suggested strategy optimize power output.

The proposed method's power output is depicted in Figure 11 (a), and it demonstrates that the suggested approach outperforms the current methods, NN, RNN, and LSTM (Rizwan et al. 2021), with a power output of 16.2. In particular, the power output for NN is 27.41, RNN is 22.65, and LSTM is 19.62. Thus, the proposed method's effectiveness is illustrated in Figure 11 (b), and it shows that the suggested approach outperforms the performance of current methods, achieving an efficiency of 95.2%. In particular, FHS attains 92.5% efficiency, while HS displays 92.8% (Huang et al. 2023). This demonstrates how much more effective the suggested approach is in reaching greater efficiency. The HGFR Control's sophisticated integration, which maximizes predictive and adaptive capabilities to improve system performance and lower losses, is responsible for this efficiency gain.

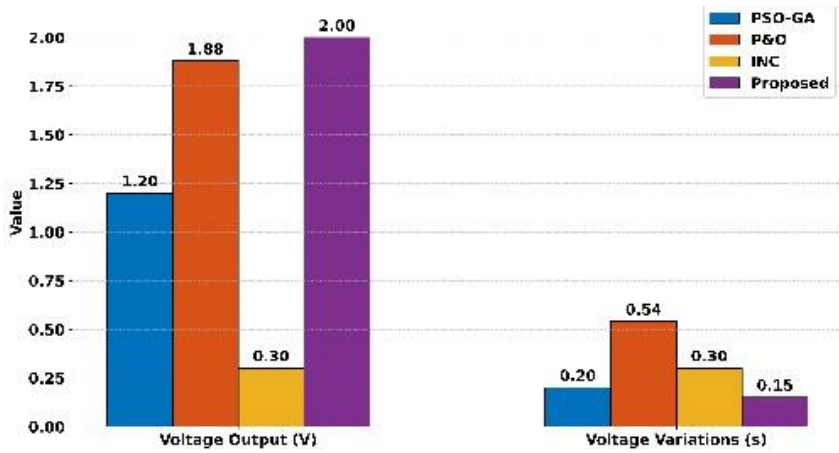

(a)

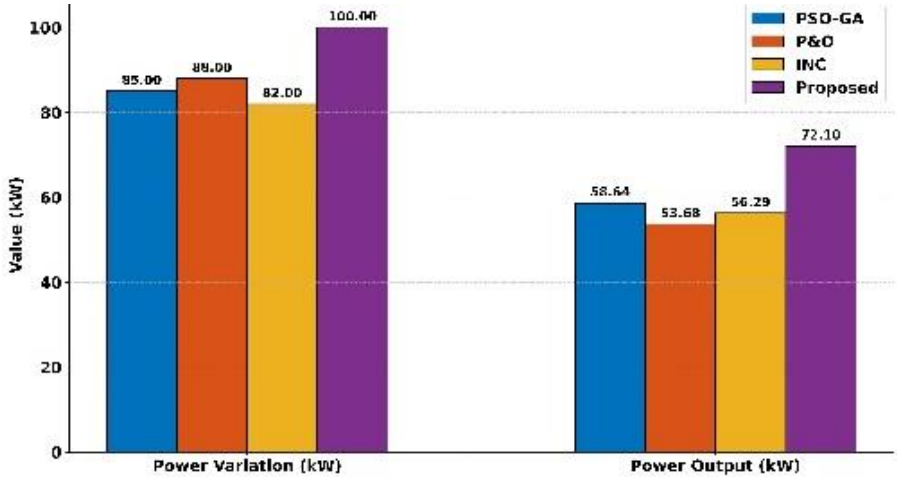

(b)

Fig. 10. (a) Comparison of Voltage Output and Voltage Variation of the proposed model, (b) Comparison of Power Variation and Power Output of the proposed model

Rys. 10. (a) Porównanie napięcia wyjściowego i zmienności napięcia proponowanego modelu, (b) Porównanie zmienności mocy i mocy wyjściowej proponowanego modelu

Moroever the standard deviation of the suggested approach is shown in Figure 11 (c). The suggested strategy provides a smaller standard deviation, indicating higher consistency and stability. In particular, FHS displays a 1.9% standard deviation compared to 2.4% for HS

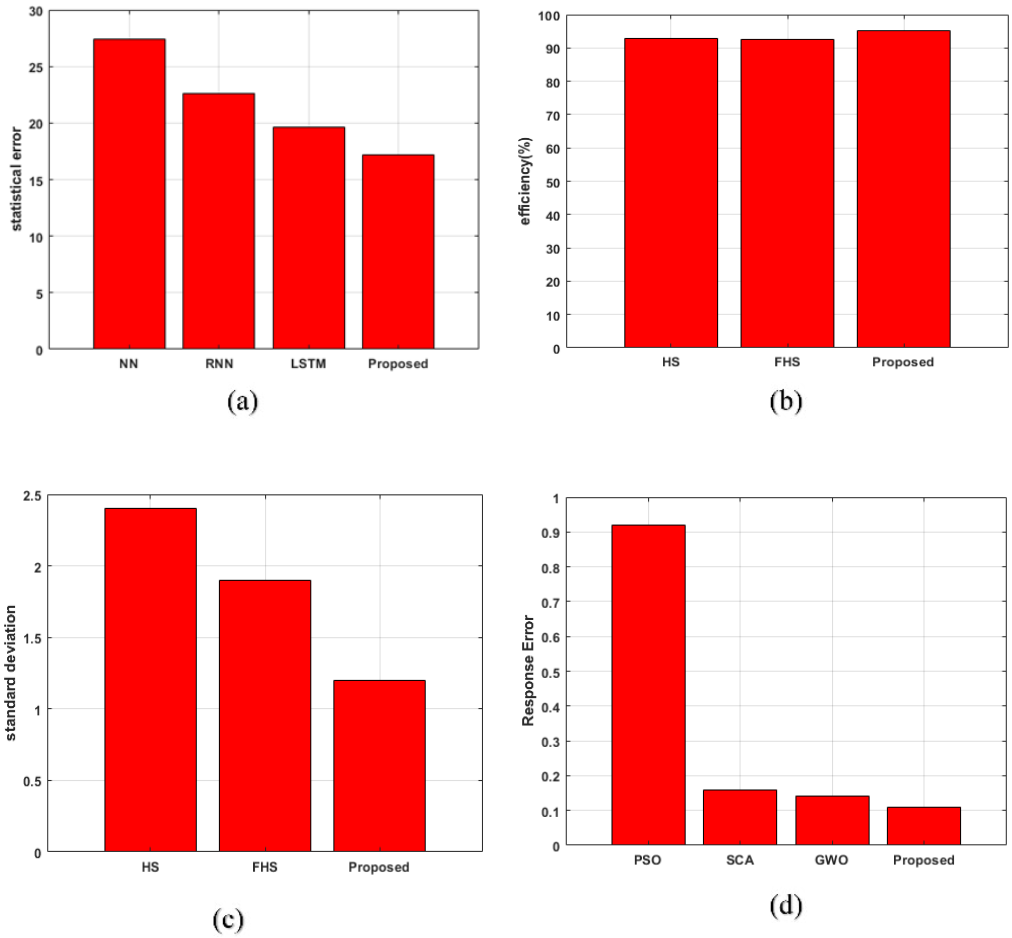

Fig. 11. (a) Comparison of Statistical Error, (b) Effieciency, (c) Standard deviation and Response error of the proposed model

Rys. 11. (a) Porównanie błędu statystycznego, (b) Efektywność, (c) Odchylenie standardowe i błąd odpowiedzi proponowanego modelu

(Huang et al. 2023). By comparison, the suggested approach shows a 1.2% lower standard deviation. This comparison demonstrates how reliable the suggested strategy is in reducing variability. Futhermore the comparison of response error between different approaches is shown in Figure 11 (d). The suggested approach performs better, with a notably decreased response error of 0.11. In comparison, PSO has a response error of 0.92, SCA 0.16, and GWO 0.142 (Xia and Wang 2024). This comparison demonstrates that the suggested HGFR Control model optimizes performance and yields more accurate outcomes by reducing response error through its clever control mechanisms.

The frequency deviation is compared across different approaches in Figure 12 (a). The graph demonstrates the performance of the proposed model, which achieves a frequency deviation of only 0.014 Hz. By comparison, PROP reports a deviation of 0.022 Hz, while TD3 and DDPG both record deviations of 0.020 Hz (Dehghani et al. 2020). The area under control for various techniques is compared in Figure 12 (b). The graph demonstrates the higher performance of the suggested strategy, which attains a noticeably bigger region under control of 3.2. By contrast, TD3 and DDPG record areas of 4.61, and PROP has an area of 4.62 (Dehghani et al. 2020). This suggests that the suggested approach is quite effective in building a system that is more stable and manageable. In contrast to earlier research, where traditional techniques frequently display wider regions signifying reduced control, the HGFR Control method dramatically enhances performance.

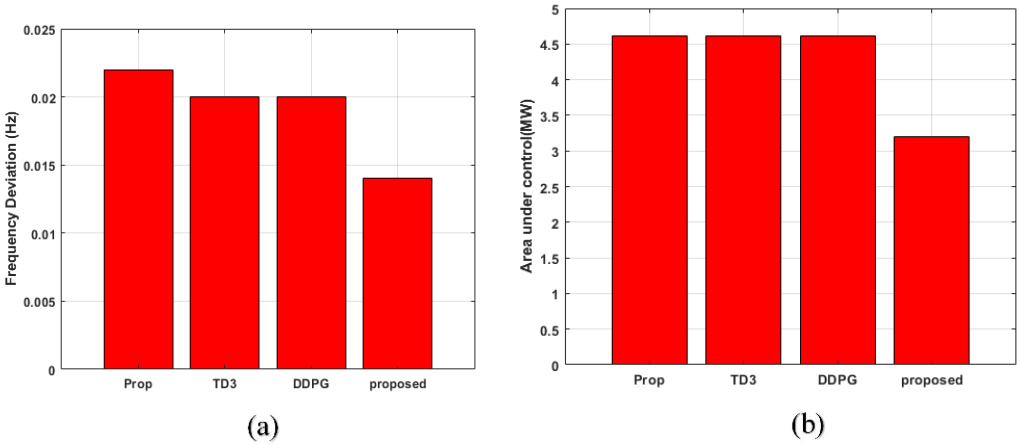

Fig.12. (a) Comparison of Frequency Deviation and (b) Area Under Control

Rys. 12. (a) Porównanie odchylenia częstotliwości i (b) Obszar pod kontrolą

4.4. Validation of the proposed model

To ensure the practical applicability and robustness of the proposed HGFR integrated with DRPG, validation studies are carried out under different disturbance scenarios in the HRES. The primary aim of this validation is to evaluate the controller's capability to mitigate power quality (PQ) issues such as voltage sag, current sag, and ramp-rate mismatches that occur due to non-linear loads and rapid variations in generation or demand. The validation process focuses on observing the dynamic behavior of voltage and current waveforms at the DC-link, source, intermediate, and load sides.

Different operating conditions are created, including sag faults and ramp-rate imbalance, to assess how effectively the proposed control framework restores system stability. The performance

is analyzed based on DC-bus voltage regulation, transient response time, current balancing, and overall PQ improvement. The results from the simulation studies clearly demonstrate that the integration of fuzzy logic, RQHO, and DRPG provides significant improvements in both transient and steady-state performance of the HRES, ensuring reliable power delivery even under adverse conditions.

Case 1: Voltage and current sag condition under HRES

In order to validate the effectiveness of the proposed HGFR with DRPG, a sag condition is created by applying non-linear load disturbances to the grid-connected HRES. During this test, the PV irradiance level is set at 1000 W/m^2, and the WT operates under a constant wind speed of 12 m/s. Under these steady input conditions, the PV system generates nearly 30 kW, while the WT contributes about 80 kW to the total power generation. The battery bank is configured to support only under-critical conditions, thereby maintaining SOC within stable limits.

When non-linear loads are connected, both voltage sag and current sag are observed at the DC-link and load side. The voltage profile exhibits a sharp sag during the initial transient interval, followed by stabilization after the corrective action of the proposed controller. Similarly, the current waveforms across source, intermediate, and load phases, and the source initially experiences high inrush current due to sudden demand mismatch, while the HGFR-DRPG controller quickly regulates intermediate currents and restores load current balance within 2 seconds.

Overall, the proposed model reveals a common trend across all three phases that is a strong initial transients with large current swings at startup, followed by a steady near-zero current region between 0.1–2.0 s, and finally the emergence of stable sinusoidal oscillations during 2.0–3.0 s. In Phase 1, the amplitudes ranged up to ±550 A initially before settling to sinusoidal currents of about ±20 A, while the load briefly dipped to –600 A. In Phase 2, the source, intermediate, and load exhibited smaller initial peaks within ±70 A, later stabilizing into sinusoidal patterns with amplitudes of ±25 A, ±18 A, and ±15 A, respectively. In Phase 3, the intermediate load rose smoothly to ±70 A during the first second, remained steady at 0 A until 2.0 s, and then oscillated sinusoidally with amplitude ±25 A.

From the results, it is validated that the proposed HGFR-DRPG control strategy successfully compensates voltage and current sags, thereby maintaining stability, reducing transient oscillations, and mitigating PQ issues in HRES. The coordinated action of shunt and series active filtering within the control algorithm ensures a continuous and stable power supply to the grid-connected load system.

Conclusion

The proposed HGFR control method for hybrid renewable energy systems integrates PV panels, wind turbines, and battery storage through a multiport DC converter. This framework addresses the critical challenges, such as inrush current surges during system start-up or reconnection and power mismatches caused by ramp-rate variations among renewable sources. The traditional control algorithms often lead to delays and instability due to the preset rule constraints and slow reactive responses. By combining RQHO with the Intelligent Hawk Fuzzy Control Algorithm, the HGFR control provides fast and precise power management, effectively resolving these issues. Additionally, the DRPG technique, which integrates GRU with DDPG, enhances forecasting accuracy and real-time adaptability and stabilizes the DC bus voltage. Thus, the simulation results demonstrate that HGFR achieves a high accuracy of 0.98, a precision of 0.92, a recall of 0.94, an F1-score of 0.91, and delivers a stable power output of 72.1 kW with minimal deviation of 1.2% and response error of 0.11. Unlike the existing methods, the proposed framework ensures faster adaptation, improved synchronization among PV, wind, and battery units, and enhanced system reliability. These results confirm that advanced control and optimization techniques overcome the limitations of traditional HRES management, ensuring efficient and stable operation at medium-scale power levels. Overall, the HGFR Control algorithm demonstrates superior performance, paving the way for more dependable and effective hybrid renewable energy systems in the future.

The Author has no conflicts of interest to declare.

Reference

Aljafari et al. 2023 – Aljafari, B., Devarajan, G., Subramani, S. and Vairavasundaram, S. 2023. Intelligent RBF-Fuzzy Controller Based Non-Isolated DC-DC Multi-Port Converter for Renewable Energy Applications. *Sustainability* 15(12), https://doi.org/10.3390/su15129425.

Alqahtani et al. 2024 – Alqahtani, B., Yang, J. and Paul, M.C. 2024. Reliability and dispatchability improvement of a hybrid system consisting of PV, wind, and bio-energy connected to pumped hydropower energy storage. *Energy Conversion and Management* 304, https://doi.org/10.1016/j.enconman.2024.118212.

Jai Andaloussi et al. 2021 – Jai Andaloussi, Z., Raihani, A., El Magri, A., Lajouad, R. and El Fadili, A. 2021. Novel nonlinear control and optimization strategies for hybrid renewable energy conversion system. *Modelling and Simulation in Engineering* 2021(1), https://doi.org/10.1155/2021/3519490.

Bashar, A. and Smys, S. 2021. Integrated renewable energy system for stand-alone operations with optimal load dispatch strategy. *Journal of Electronics* 3(02), pp. 89–98, https://doi.org/10.36548/jei.2021.2.002.

Benadli et al. 2021 – Benadli, R., Bjaoui, M., Khiari, B. and Sellami, A. 2021. Sliding mode control of hybrid renewable energy system operating in grid connected and stand-alone mode. *Power Electronics and Drives* 6(1), pp. 144–166, https://doi.org/10.2478/pead-2021-0009.

Das et al. 2021 – Das, B.K., Tushar, M.S.H. and Hassan, R. 2021. Techno-economic optimisation of stand-alone hybrid renewable energy systems for concurrently meeting electric and heating demand. *Sustainable Cities and Society* 68, https://doi.org/10.1016/j.scs.2021.102763.

Dehghani et al. 2020 – Dehghani, M., Taghipour, M., Gharehpetian, G.B. and Abedi, M. 2020. Optimized fuzzy controller for MPPT of grid-connected PV systems in rapidly changing atmospheric conditions. *Journal of Modern Power Systems and Clean Energy* 9(2), pp. 376–383, https://doi.org/10.35833/MPCE.2019.000086.

Foti et al. 2021 – Foti, S., Testa, A., De Caro, S., Tornello, L.D., Scelba, G. and Cacciato, M. 2021. Multi-level multi-input converter for hybrid renewable energy generators. *Energies* 14(6), https://doi.org/10.3390/en14061764.

Heenkenda et al. 2023 – Heenkenda, A., Elsanabary, A., Seyedmahmoudian, M., Mekhilef, S., Stojcevski, A. and Ab Aziz, N.F. 2023. Unified power quality conditioners based different structural arrangements: A comprehensive review. *IEEE Access* 11, pp. 43435–43457, https://doi.org/10.1109/ACCESS.2023.3269855.

Hossain et al. 2021 – Hossain, M.A., Chakrabortty, R.K., Elsawah, S., Gray, E.M. and Ryan, M.J. 2021. Predicting wind power generation using hybrid deep learning with optimization. *IEEE Transactions on Applied Superconductivity* 31(8), pp. 1–5, https://doi.org/10.1109/TASC.2021.3091116.

Huang et al. 2023 – Huang, N., Wang, S., Wang, R., Cai, G., Liu, Y. and Dai, Q. 2023. Gated spatial-temporal graph neural network based short-term load forecasting for wide-area multiple buses. *International Journal of Electrical Power & Energy Systems* 145, https://doi.org/10.1016/j.ijepes.2022.108651.

Karthikeyan, N. and Jebaselvi, G.A. 2024. A bidirectional four-port DC–DC converter for grid connected and isolated loads of hybrid renewable energy system using hybrid approach. *Analog Integrated Circuits and Signal Processing* 118(3), pp. 467–487, https://doi.org/10.1007/s10470-024-02251-6.

Kumar, G.A. and Shivashankar, 2022. Optimal power point tracking of solar and wind energy in a hybrid wind solar energy system. *International Journal of Energy and Environmental Engineering* 13(1), pp. 77–103, https://doi.org/10.1007/s40095-021-00399-9.

Liu et al. 2022 – Liu, S., You, H., Liu, Y., Feng, W. and Fu, S. 2022. Research on optimal control strategy of wind–solar hybrid system based on power prediction. *ISA Transactions* 123, pp. 179–187, https://doi.org/10.1016/j.isatra.2021.05.010.

Ma, J. and Liu, F. 2022. Bearing fault diagnosis with variable speed based on fractional hierarchical range entropy and hunter–prey optimization algorithm–optimized random forest. *Machines* 10(9), https://doi.org/10.3390/machines10090763.

Mahmoud et al. 2022 – Mahmoud, F.S., Diab, A.A.Z., Ali, Z.M., El-Sayed, A.H.M., Alquthami, T., Ahmed, M. and Ramadan, H.A. 2022. Optimal sizing of smart hybrid renewable energy system using different optimization algorithms. *Energy Reports* 8, pp. 4935–4956, https://doi.org/10.1016/j.egyr.2022.03.197.

Mahmoudi et al. 2021 – Mahmoudi, S.M., Maleki, A. and Ochbelagh, D.R. 2021. Optimization of a hybrid energy system with/without considering back-up system by a new technique based on fuzzy logic controller. *Energy Conversion and Management* 229, https://doi.org/10.1016/j.enconman.2020.113723.

Moghaddam et al. 2023 – Moghaddam, M.J.H., Bayat, M., Mirzaei, A., Nowdeh, S.A. and Kalam, A. 2023. Multiobjective and Simultaneous Two-Problem Allocation of a Hybrid Solar-Wind Energy System Joint with Battery Storage Incorporating Losses and Power Quality Indices. *International Journal of Energy Research* 2023(1), https://doi.org/10.1155/2023/6681528.

Nuvvula et al. 2021 – Nuvvula, R.S., Devaraj, E. and Teegala, S.K. 2021. A hybrid multiobjective optimization technique for optimal sizing of BESS-WtE supported multi-MW HRES to overcome ramp rate limitations on thermal stations. *International Transactions on Electrical Energy Systems* 31(12), https://doi.org/10.1002/2050-7038.13241.

Pangedaiah et al. 2021 – Pangedaiah, B., Obulesu, Y.P. and Kota, V.R. 2021. A new architecture topology for back to back grid-connected hybrid wind and PV system. *Journal of Electrical Engineering & Technology* 16(3), pp. 1457–1467, https://doi.org/10.1007/s42835-021-00685-w.

Parvaneh, M.H. and Khorasani, P.G. 2020. A new hybrid method based on fuzzy logic for maximum power point tracking of photovoltaic systems. *Energy Reports* 6, pp. 1619–1632, https://doi.org/10.1016/j.egyr.2020.06.010.

Singh et al. 2024 – Singh, S., Subburaj, V., Sivakumar, K., Anil Kumar, R., Muthuramam, M.S., Rastogi, R., Ratansing Patil, V. and Rajaram, A. 2024. Optimum power forecasting technique for hybrid renewable energy systems using deep learning. *Electric Power Components and Systems*, pp. 1–18, https://doi.org/10.1080/15325008.2024.2316251.

Paulsamy, K. and Karuvelam, S. 2025. Modeling and Design of a Grid-Tied Renewable Energy System Exploiting Re-Lift Luo Converter and RNN Based Energy Management. *Sustainability* 17(1), https://doi.org/10.3390/su17010187.

Rajasekaran, R. and Rani, P.U. 2021. Combined HCS–RBFNN for energy management of multiple interconnected microgrids via bidirectional DC–DC converters. *Applied Soft Computing* 99, https://doi.org/10.1016/j.asoc.2020.106901.

Rosales-Asensio et al. 2021 – Rosales-Asensio, E., Rosales, A.E. and Colmenar-Santos, A. 2021. Surrogate optimization of coupled energy sources in a desalination microgrid based on solar PV and wind energy. *Desalination* 500, https://doi.org/10.1016/j.desal.2020.114882.

Rizwan et al. 2021 – Rizwan, M., Hong, L., Muhammad, W., Azeem, S.W. and Li, Y. 2021. Hybrid Harris Hawks optimizer for integration of renewable energy sources considering stochastic behavior of energy sources. *International Transactions on Electrical Energy Systems* 31(2), https://doi.org/10.1002/2050-7038.12694.

Samy et al. 2021 – Samy, M.M., Elkhouly, H.I. and Barakat, S. 2021. Multi-objective optimization of hybrid renewable energy system based on biomass and fuel cells. *International Journal of Energy Research* 45(6), pp. 8214–8230, https://doi.org/10.1002/er.5815.

Saber et al. 2021 – Saber, H., Mazaheri, H., Ranjbar, H., Moeini-Aghtaie, M. and Lehtonen, M. 2021. Utilization of in-pipe hydropower renewable energy technology and energy storage systems in mountainous distribution networks. *Renewable Energy* 172, pp. 789–801, https://doi.org/10.1016/j.renene.2021.03.072.

Sahu et al. 2020 – Sahu, P.C., Prusty, R.C. and Sahoo, B.K. 2020. Modified sine cosine algorithm-based fuzzy-aided PID controller for automatic generation control of multiarea power systems. *Soft Computing* 24(17), pp.12919-12936, https://doi.org/10.1007/s00500-020-04716-y.

Xia, S. and Wang, C. 2024. Energy Management for Hybrid Energy Storage System in Electric Based on Deep Deterministic Policy Gradient. *International Journal of Computer Science and Information Technology* 2(1), pp. 198–207, https://doi.org/10.62051/ijcsit.v2n1.22.

Vadivel, S. and Ragupathy, U.S. 2021. Modeling and design of high performance converters for optimal utilization of interconnected renewable energy resources to micro grid with GOLRS controller. *International Journal of Control, Automation and Systems* 19, pp. 63–75, https://doi.org/10.1007/s12555-019-0498-2.

Xie et al. 2021 – Xie, J., Tuffner, F.K., Elizondo, M.A. and Schneider, K.P. 2021. Modeling and simulation of inrush currents in harmonic domain. *2021 IEEE Power & Energy Society Innovative Smart Grid Technologies Conference* (*ISGT*), pp. 1–5, https://doi.org/10.1109/ISGT49243.2021.9372259.

Renganathan Rani Hemamalini

Poprawa dopasowania mocy i wydobycia energii w hybrydowych systemach energii odnawialnej dzięki zastosowaniu koncepcji sterowania rekurencyjnego HawkDeep Gradient Fuzzy Recurrent Control

Streszczenie

Hybrydowe systemy energii odnawialnej są jednym z najbardziej odpowiednich rozwiązań dla rosnącego zapotrzebowania na energię. Jednak na ich wydajność znaczący wpływ mają nierównowaga mocy, niestabilne napięcie szyny prądu stałego oraz zmniejszona wydajność systemu. Aby rozwiązać te problemy, zaproponowano nowatorską strukturę HawkDeep Gradient Fuzzy Recurrent Control. Metoda ta służy do optymalizacji zarządzania charakterystyką mocy i stabilizacji wydajności systemu w systemach o wysokim udziale energii odnawialnej. Ponadto obecne algorytmy sterowania często opierają się na z góry określonych regułach, które nie są wystarczająco elastyczne, aby poradzić sobie z nagłymi i nieregularnymi zmianami zapotrzebowania na energię i jej wytwarzania. Aby rozwiązać ten problem, zaproponowano inteligentny algorytm sterowania Hawk Fuzzy, który integruje logikę rozmytą z optymalizacją Reflective Quasi-Hawk w celu szybkiego uzyskania najlepszych odpowiedzi, gwarantując w ten sposób zrównoważone dostawy energii i zapotrzebowanie na nią, nawet w przypadku nagłych prądów rozruchowych. Ponadto niedopasowanie szybkości narastania powoduje tymczasową nierównowagę mocy i niestabilność napięcia szyny prądu stałego, obciążając system i zmniejszając jego wydajność. W związku z tym wprowadzono technikę głębokiego rekurencyjnego gradientu polityki, która łączy bramkowane jednostki rekurencyjne z głębokim deterministycznym gradientem polityki. Metoda optymalizuje działania sterujące w celu stabilnej regulacji mocy, w której bramkowane jednostki rekurencyjne zajmują się dynamiką czasową w celu skorygowania rozbieżności w szybkości narastania i nierównowagi mocy w wieloportowych przetwornikach prądu stałego. Wyniki eksperymentów pokazują, że proponowany model osiąga dokładność 0,98 i moc wyjściową netto 72,1 kW w zmiennych warunkach, zapewniając wydajną i stabilną pracę przy średnich poziomach mocy.

Słowa kluczowe: stabilność mikrosieci, przetworniki, panele fotowoltaiczne, energia alternatywna, zdecentralizowane wytwarzanie energii